Temperature-Independent Vibrational Dynamics in an Organic Photovoltaic Material

ARTICLE *in* THE JOURNAL OF PHYSICAL CHEMISTRY B · SEPTEMBER 2010

Impact Factor: 3.3 · DOI: 10.1021/jp105772y · Source: PubMed

3 AUTHORS, INCLUDING:

Ryan D. Pensack
Princeton University
25 PUBLICATIONS **367** CITATIONS

SEE PROFILE

Temperature-Independent Vibrational Dynamics in an Organic Photovoltaic Material

Ryan D. Pensack, Kyle M. Banyas, and John B. Asbury*

Department of Chemistry The Pennsylvania State University, University Park, Pennsylvania 16802

Received: June 22, 2010; Revised Manuscript Received: August 16, 2010

Ultrafast orientational motion and spectral diffusion of the carbonyl stretch vibration of the functionalized fullerene, PCBM, blended with the conjugated polymer, CN-MEH-PPV, are examined with two-dimensional infrared and polarization-resolved IR pump probe spectroscopy. In previous contributions from our group, the carbonyl stretch frequency of PCBM has been used as a local vibrational reporter to measure the temperature dependence of the time scale for dissociation of charge transfer excitons in CN-MEH-PPV:PCBM polymer blends. It was found that the rate of charge separation is independent of temperature, indicating that charge separation occurs through an activationless pathway. This assignment was supported by the observation at room temperature that thermal fluctuations do not give rise to spectral diffusion of the carbonyl stretch vibration on the picosecond and longer time scale. In this contribution, we examine the temperature dependence of the carbonyl vibrational dynamics to determine whether thermal fluctuations might give rise to spectral diffusion at other temperatures. We find that the time scale for fast wobbling-in-cone orientational motion is independent of temperature on the subpicosecond time scale. Similarly, spectral diffusion is not observed on the picosecond and longer time scale at all temperatures examined confirming our earlier interpretation of the frequency shift dynamics exclusively in terms of charge separation. Interestingly, the half angle characterizing the wobbling-in-cone orientational motion does increase at higher temperature due to increased free-volume resulting from thermal expansion of the polymer blend.

Introduction

The first steps leading to solar energy conversion in photovoltaic devices are absorption of solar photons followed by formation of separated electrons and holes. In organic solar cells, the initial electronic excitations formed by absorption of light are Frenkel-like excitons that consist of electron−hole pairs strongly bound to the same conjugated segment.[1−3] There is evidence to suggest that these initial excitons form charge transfer (CT) excitons at electron donor/acceptor interfaces by electron transfer from the donor to the acceptor.[4,5] Dissociation of these CT excitons has become a topic of considerable interest because the process has been recognized as a limiting step in the charge photogeneration efficiency of certain organic photovoltaic (OPV) materials.[6−9] Electron−hole pairs in CT excitons are expected to be bound together by their mutual Coulombic attraction, which has been estimated to be several tenths of an electronvolt (eV).[6,10−13]

We recently reported activationless charge separation in a polymer blend of CN-MEH-PPV with PCBM (structures depicted in Figure 1A) on the basis of a temperature-dependent study of the time evolution of the vibrational spectra of the carbonyl stretch of PCBM following visible excitation.[14−16] The carbonyl stretch vibration exhibits a shift to lower frequency as electrons that are initially transferred to PCBM molecules at the interfaces of PCBM clusters diffuse into the interiors of the clusters (Figure 1B).[17,18] This motion results in a shift of the carbonyl spectrum because molecules residing at interfaces of PCBM clusters have higher frequency carbonyl vibrations in comparison with molecules in the interiors of the clusters (Figure 1C). The correlation between vibrational frequency and radial position results from a combination of solvatochromism[19] and a vibrational Stark shift.[20,21] A study of the rate of the photoinduced carbonyl frequency shift at several temperatures demonstrated that the rate of the shift was independent of temperature.[14]

The assignment of activationless charge separation on the basis of temperature independent frequency shift dynamics in ref 14 is predicated on the observation that the time-dependent frequency shifts in the transient vibrational spectra arise exclusively from charge separation rather than from alternate sources of spectral evolution.[17,18,22,23] Examples of alternate sources of spectral evolution include interference from excited state species or photoproducts, thermal effects as a result of optical pump energy redistribution, and spectral diffusion due to equilibrium fluctuations. We refer the reader to the relevant publications demonstrating that no excited state or photoproduct species absorb in this spectral window on ultrafast time scales in this system[18,23] and that thermal redistribution does not result in significant shifts of the carbonyl bleach spectra.[17] We previously demonstrated that equilibrium fluctuations do not contribute to spectral diffusion at room temperature on the picosecond and longer time scale in this system.[17] Equilibrium fluctuations do give rise to wobbling-in-cone[24,25] orientational motion of the carbonyl bonds on the few hundred femtosecond time scale at room temperature.[26] We wished to investigate whether the time scale for wobbling-in-cone orientational motion is temperature-dependent in this system to determine whether the rate of this motion might decrease at low temperature, possibly giving rise to spectral diffusion on the picosecond time scale.

In this contribution, we report temperature-dependent dynamics of excited state relaxation, orientational motion, and spectral diffusion of the carbonyl stretch vibration of PCBM in a 1:1 (by mass) polymer blend of CN-MEH-PPV with PCBM using ultrafast vibrational spectroscopy. We find that the time scale of orientational motion is independent of temperature between

* Corresponding author. E-mail: jasbury@psu.edu.

10.1021/jp105772y
Published on Web 09/02/2010

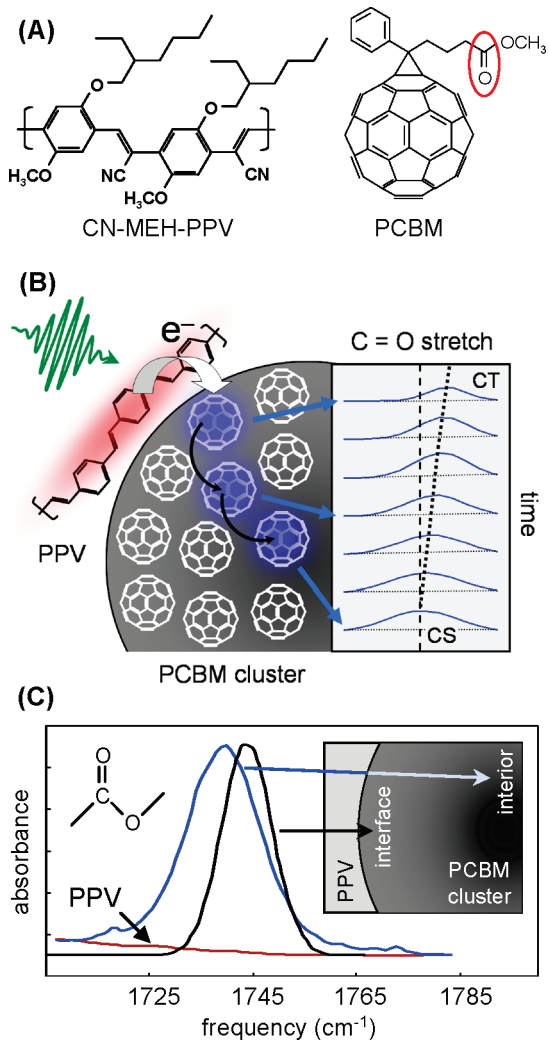

Figure 1. (A) Molecular structures of CN-MEH-PPV and PCBM. (B) Ultrafast vibrational spectroscopy was used to measure the separation of CT excitons at polymer/PCBM interfaces through the time evolution of the carbonyl stretch frequency (see ref 16). (C) The frequency evolution of the carbonyl stretch of PCBM can be used to probe CT exciton dissociation because the frequency of the vibrational mode is sensitive to the position of PCBM molecules relative to the polymer/PCBM interfaces.

200 and 350 K, indicating that this motion is not activated, but inertial in nature. The wobbling-in-cone orientational motion is complete on the subpicosecond time scale at all temperatures investigated. We also observe that spectral diffusion does not occur on the picosecond and longer time scale at all temperatures examined, which confirms our earlier interpretation of the photoinduced frequency shift dynamics of the carbonyl stretch mode following ultrafast visible excitation exclusively in terms of charge separation.[14,17,18] The spectral diffusion dynamics are independent of temperature because changes of frequency require center-of-mass motion of PCBM molecules, which is expected to be extremely slow in this system. We do observe an increase in the cone half angle of wobbling-in-cone orientational motion with increased temperature that is indicative of an increase in the free volume at higher temperature. The increase in free volume is associated with thermal expansion at elevated temperatures[27] as a result of enhanced conformational entropy within the material.

Experimental Section

Ultrafast polarization resolved infrared (IR) pump−probe experiments are conducted using an ultrafast Ti:sapphire laser (Quantronix, Integra-CE) that pumps an optical parametric amplifier (OPA). The OPA is used to generate mid-IR pulses at 5.8 μm with 6 μJ pulse energy and 100 fs duration that serve as both the pump and the probe for the polarization resolved IR experiments. The IR pulses from the first OPA are split into two pulses with a 30:1 intensity ratio. The less intense probe pulse is focused at the sample with a 200 μm diameter spot size. The probe is dispersed in a spectrograph and detected with a 64-element mercury cadmium telluride dual array detector (Infrared Systems/Infrared Associates) to capture 32 probe frequencies simultaneously while facilitating single shot normalization. The optical path for polarization-resolved IR experiments was designed on the basis of work reported recently by Tan, Piletic, and Fayer.[28] Prior to impinging on the last steering mirror before the sample, the probe pulse passes through a wire-grid polarizer. After interacting with the sample and before the next steering mirror, the probe pulse passes through another wire-grid polarizer that is mounted in a computer controlled rotation stage. The rotation stage permits automated toggling during data collection between horizontal and vertical probe polarizations that are transmitted to the spectrograph. In this way, the anisotropy can be precisely determined and is not influenced by laser drift because both polarizations are collected simultaneously. The polarization angle of the first polarizer in the probe path is set such that equal intensities are observed on the array detector when measured with horizontal or vertical polarization. The more intense pump pulse also passes through a polarizer just before the last steering mirror prior to impinging on the sample, thus ensuring maximum polarization purity in the experiments. The pump spot size at the sample is 250 μm diameter.

Two-dimensional infrared (2D IR) experiments are performed with the two pulse self-heterodyned pump−probe approach[26,29] using the laser system described above. The probe pulse is identical to that used in the polarization-resolved IR experiments. Before encountering the polarizer, the pump pulse passes through a Fabry−Perot interferometer to create a continuously adjustable pump spectrum with a full width at half-maximum (fwhm) of ~8 cm^{-1} that is stabilized to within ±1 cm^{-1}. The spectrum transmitted through the interferometer is measured periodically during data collection to ensure that the pump frequency is precisely controlled during the experiment. Both experiments utilize a reflective sample geometry such that the pump and probe beams do not encounter window materials in their overlap region. This geometry largely eliminates nonresonant signals and permits us to analyze the transient spectra and kinetics near the time origin of the experiment.

The polymer blend is prepared by codissolving the functionalized fullerene, PCBM (Aldrich), and the conjugated polymer, CN-MEH-PPV (American Dye Source), in chlorobenzene at a mass ratio of 1:1. The chlorobenzene solution is drop-cast onto a silver mirror and spun at 80 rpm to ensure uniform drying. The resulting film is 3 μm thick and is uniform throughout its cross section as determined by SEM imaging.[17] As reported previously,[17] the morphology of the polymer blend is characterized by 50−100 nm clusters of PCBM that are imbedded in a matrix of CN-MEH-PPV. The sample is mounted on a cold-finger in an evacuated cryostat for all experiments reported here.

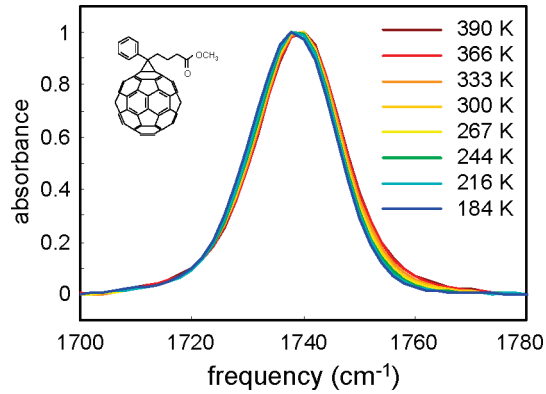

Figure 2. Comparison of temperature-dependent linear IR spectra of the carbonyl group of PCBM blended with CN-MEH-PPV. The spectra display a small shift to lower frequency with lower temperature that is indicative of increased dipolar coupling between carbonyl groups.

Results

Figure 2 displays a comparison of linear IR spectra of the 1:1 CN-MEH-PPV:PCBM polymer blend recorded at temperatures ranging from 184 to 390 K in the region of the carbonyl stretch vibration of the methyl ester group of PCBM. Eight normalized spectra at differing temperatures are displayed together on the same frequency axis. The comparison reveals that the carbonyl stretch center frequency shifts about 1.5 cm^{-1} to higher values as the temperature is increased from 184 to 390 K. About one-third of this shift occurs between temperatures of 300 and 390 K, as reported previously.[17] The fwhm of the vibrational line shape of the carbonyl absorption feature changes less than 0.3 cm^{-1} over the same temperature range. The line shape does become slightly asymmetric at lower temperature, with a corresponding loss of absorption preferentially around 1760 cm^{-1}.

To explore the vibrational dynamics, polarization-resolved IR pump probe transient spectra were collected in the region of the carbonyl stretch of PCBM and are displayed in Figure 3A as a two-dimensional frequency-time contour plot. The IR pump pulse used in the experiment was centered on the ground-to-first-excited-state transition (0−1) of the carbonyl stretch mode at 1740 cm^{-1}. The transient spectra displayed in the contour plot were collected with parallel pump and probe polarizations at 300 K and are normalized to the maximum positive signal. Contours are displayed at 10% intervals except around zero signal amplitude, where they appear at 1% intervals. The peak appearing with a maximum around 1740 cm^{-1} near the time origin corresponds to the 0−1 transition, and the peak appearing around 1720 cm^{-1} results from the first-to-second-excited-state transition (1−2). The decay of both peaks with increasing time delay corresponds to vibrational relaxation of the first excited state. Figure 3B displays one-dimensional slices from the contour plot in Figure 3A. The slices represent transient vibrational spectra with corresponding time delays of 0.1 and 10 ps following excitation of the sample by the ultrafast IR pump pulse. The 0.1 ps spectrum depicts the vibrational features resulting from excitation of the 0−1 transition of the carbonyl stretch mode of PCBM. The center frequency and line shape correspond closely to the vibrational transition in the linear IR spectra displayed in Figure 2. The vibrational features in the 10 ps spectrum appear shifted to higher frequencies in comparison with the 0.1 ps spectrum. The frequency shift with time is indicated in the contour plot by the dashed lines overlapping the 0−1 and 1−2 transitions.

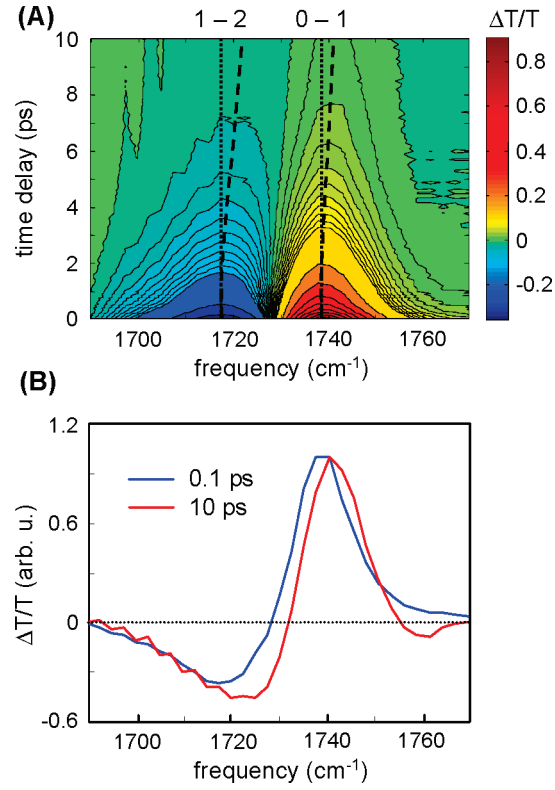

Figure 3. (A) Polarization-resolved IR pump−probe spectra plotted versus the corresponding time delay in a 2D freq−time plot. The data were collected with parallel polarizations at 300 K. Contours appear at 10% intervals except around zero signal amplitude, where they are displayed at 1% intervals. (B) Comparison of transient vibrational spectra measured at 0.1 and 10 ps time delays. The spectra show the shift of the 0−1 and 1−2 transitions to higher frequencies at longer time delays.

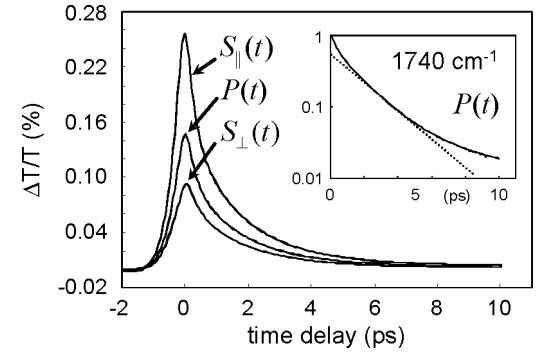

Figure 4. Comparison of IR pump−probe kinetics traces measured at 1740 cm^{-1} with parallel, $S_{\parallel}(t)$, and perpendicular, $S_{\perp}(t)$, polarizations at 300 K. These measurements are combined to construct the population relaxation kinetics trace, $P(t)$, that is not influenced by orientational motion of the carbonyl groups. (Inset) Population relaxation trace displayed in a semilogarithmic plot. In this representation, a single-exponential decay would appear as the dotted line. The curvature of the data indicates nonsingle-exponential behavior.

To further explore the origin of the frequency shift of the vibrational features appearing in Figure 3, we examined the excited state relaxation dynamics of the carbonyl stretch of PCBM following ultrafast excitation of the 0−1 transition. Polarization resolved IR pump−probe kinetics traces measured from the center of the 0−1 transition at 1740 cm^{-1} at a temperature of 300 K are displayed in Figure 4. The kinetics traces were collected with parallel, $S_{\parallel}(t)$, and perpendicular, $S_{\perp}(t)$, pump and probe polarizations. These traces are combined to construct the population relaxation kinetics, $P(t)$, according to

$$P(t) = \frac{1}{3}(S_{\parallel}(t) + 2S_{\perp}(t)) \quad (1)$$

which removes the influence of orientational motion of the carbonyl groups. The inset of Figure 4 displays the population relaxation kinetics trace from the main panel on a semilogarithmic plot. In this representation, a single-exponential decay appears as a straight line with the negative slope equal to the time constant of the decay (see dotted line in the inset). The data demonstrate that the excited state relaxation dynamics of the carbonyl mode of PCBM do not follow single-exponential behavior.

The population relaxation kinetics trace displayed in Figure 4 is fit with a model function, $F_P(t)$, similar to our earlier report,[26] in which the signal at negative time delays (probe pulse arriving before the pump pulse) is fit with a time-domain analog of a pseudovoight function, $S_{FID}(t)$, to describe the perturbed free induction decay of the carbonyl stretch vibration. In contrast to our earlier kinetic model, however, the population relaxation dynamics are fit with a triexponential function, $C_1(t)$, at positive time delays to account for a vibrationally hot intermediate state that forms after excited state relaxation (see Discussion section for details),

$$\begin{aligned} F_P(t) &= A\int_{-\infty}^{\infty} [S_{FID}(t+\tau)\,\Theta(-t-\tau) + C_1(t+\tau)\,\Theta(t+\tau)]\,G(\tau)\,d\tau \\ C_1(t) &= (1 - a_s - a_{pp})\exp(-t/\tau_f) + a_s\exp(-t/\tau_s) + a_{pp}\exp(-t/\tau_{pp}) \\ S_{FID}(t) &= (1-b)\exp(-t^2/2\sigma_{FID}{}^2) + b\exp(-2|t|/\sigma_{FID}) \end{aligned} \quad (2)$$

The fitting function is convolved with a 150 fs Gaussian instrument response function, $G(t)$, to account for the finite time resolution of the experiment. The Heaviside step function, $\Theta(t)$, toggles between the perturbed free induction decay and the population relaxation functions in the calculation. The curve corresponding to the best fit (from a least-squares fitting procedure) using the model function with the triexponential decay is overlaid on the population decay trace in the main panel of Figure 4 and the inset. The data and fit curves are indistinguishable. The lifetimes and amplitudes of decay components of the triexponential function obtained from the best fit are represented in Table 1 in the section labeled "300 K". The term, A, in eq 2 is a parameter to fit the amplitude of the population decay traces. The longest time-scale component with lifetime τ_{pp} varies slowly over the 10 ps time window and is used to account for the small residual signal at long time delays. The time constant for this component is not precisely determined from the data. The error limits appearing in Table 1 were determined by fixing the parameter in question at a range of values while allowing all other parameters in eq 2 to vary in the least-squares procedure such that the sum of the squares of the residuals increased by 50% relative to the best fit. Repeated measurements of the population relaxation traces were identical within experimental precision and are in close agreement with our earlier report.[26]

The curvature in the population relaxation kinetics trace on the 5−10 ps time scale in the inset of Figure 4 indicates that the decay of the vibrational feature transitions from a process with a time constant of a few picoseconds to one with a much longer time constant. The spectral features associated with the longest-lived transient species are represented in the 10 ps spectrum in Figure 3B. To explore the origin of the nonexponential behavior on the picosecond time scale, we subtracted the long time-scale exponential component obtained from the fitting procedure with time constant, τ_{pp}, from the population relaxation kinetics trace at 1740 cm^{-1}. The resulting population relaxation trace with the long time-scale component subtracted is displayed on a semilogarithmic plot in Figure 5.

TABLE 1: Best Fit Parameters for Population Relaxation Dynamics, $C_1(t)$, of the Carbonyl Stretch of PCBM

temp, K	τ_f (ps)	τ_s (ps)	a_s (%)	τ_{pp} (ps)	a_{pp} (%)
350	0.31	1.67	60	50	1.9
error limits: upper	0.37	1.77	64	NA	2.6
lower	0.27	1.50	55		1.6
300	0.28	1.69	57	50	3.5
error limits: upper	0.33	1.81	61	NA	4.0
lower	0.24	1.54	52		3.0
250	0.28	1.78	53	50	2.7
error limits: upper	0.33	1.92	56	NA	3.3
lower	0.24	1.65	48		2.2
200	0.28	1.92	50	50	2.5
error limits: upper	0.32	2.11	55	NA	2.9
lower	0.25	1.79	47		1.1

Population relaxation traces at three other frequencies, 1751, 1746, and 1735 cm^{-1}, were processed in a similar manner and are displayed in Figure 5, as well. The kinetics traces have been normalized to their maximum signal at zero time delay. The data reveal biphasic excited state relaxation dynamics that consist of a subpicosecond component comprising ~40% of the decay and a 1.69 ps (rounded to 1.7 ps) component that is independent of probe frequency. The dotted line in Figure 5 represents the appearance of a single-exponential decay with a time constant of 1.7 ps. The observation of a frequency-independent excited state lifetime contrasts with our earlier assignment of a wavelength-dependent excited state lifetime in this system.[26]

Figure 6 displays the time-dependent anisotropy of the carbonyl stretch mode of PCBM measured at 1740 cm^{-1} at temperatures of 200, 250, 300, and 350 K. The orientational motion of isotropically distributed transition dipole moments is characterized by the time-dependent anisotropy, $r(t)$. The anisotropy is calculated from polarization-resolved IR pump−probe kinetics traces according to

$$r(t) = 0.4C_2(t) = (S_{\parallel}(t) - S_{\perp}(t))/(S_{\parallel}(t) + 2S_{\perp}(t)) \quad (3)$$

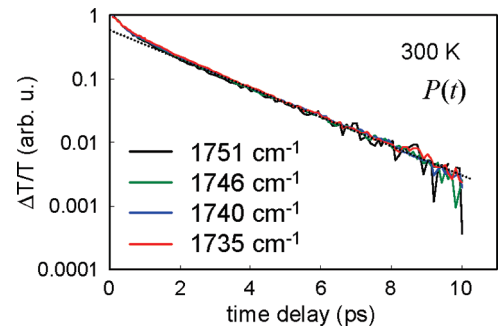

Figure 5. Comparison of population relaxation traces at several frequencies around 1740 cm^{-1} after subtracting the long-time-scale decay component obtained from the fitting procedure. The data indicate that the excited state relaxation rate is frequency-independent.

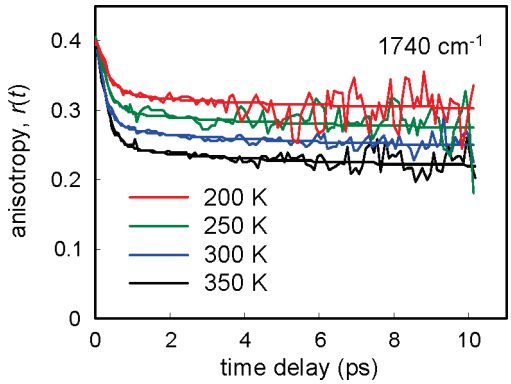

Figure 6. Comparison of anisotropy decay dynamics measured at 1740 cm^{-1} for all temperatures examined. The time scale for wobbling-in-cone orientational motion does not change with temperature. However, the wobbling-in-cone angle does increase with temperature due to thermal expansion of the polymer blend.

where $C_2(t)$ is the orientational correlation function. The transient vibrational signals, $S_{\parallel}(t)$ and $S_{\perp}(t)$, are measured with parallel and perpendicular pump and probe polarizations, respectively. Kinetics traces from which the anisotropy at 300 K is calculated are displayed in Figure 4. Because we use a reflective sample geometry that minimizes nonresonant contributions to the IR pump−probe signals,[18,26] the anisotropy of the carbonyl stretch mode can be calculated at all time delays. Consequently, we plot the anisotropy beginning at the time origin of the experiment. Since our first report of the orientational motion of the carbonyl stretch mode,[26] we have added an automated rotation stage to toggle between measurements of parallel and perpendicular polarization traces as the data are collected, thereby eliminating potential errors in the measured anisotropy values that may arise from laser drift as one polarization kinetics trace is measured after the other. The initial anisotropy value of 0.34 reported previously may have been influenced by laser drift of this type because our earlier experimental implementation did not include the automated rotation stage.

To quantify the temperature dependence of the orientational diffusion dynamics, the polarization-resolved IR pump probe kinetics traces measured at 1740 cm^{-1} were fit with the model function, $F_{OR}(t)$, that accounts for all population relaxation and orientational diffusion dynamics simultaneously,

$$F_{OR}(t) = A\int_{-\infty}^{\infty} [S_{FID}(t+\tau)\,\Theta(-t-\tau) + C_1(t+\tau)\,\Theta(t+\tau)](1 + xC_2(|t+\tau|))\,G(\tau)\,d\tau \quad (4)$$

Parameters for the population relaxation dynamics, $C_1(t)$, and perturbed free induction decay, $S_{FID}(t)$, functions were derived from the results of fitting the population relaxation kinetics calculated for each temperature according to eq 2 (see data displayed in Figure 4 for an example at 300 K). Parameters for the population relaxation dynamics are summarized in Table 1 for each temperature. The parameter, x, has values of 0.8 or −0.4, depending on whether the function is used to fit data collected with parallel or perpendicular pump and probe polarizations, respectively. The orientational correlation function was modeled as a triexponential function according to

$$C_2(t) = (Q^2 + (1 - Q^2)\exp(-t/\tau_w))[(1 - a_{or}) \times \exp(-t/\tau_1) + a_{or}\exp(-t/\tau_2)] \quad (5)$$

TABLE 2: Best Fit Parameters for Orientational Correlation Function, $C_2(t)$, of the Carbonyl Stretch of PCBM

temp, K	τ_w (ps)	τ_1 (ps)	Q^2 (%)	τ_2 (ps)	a_{or} (%)	θ (°)
350	0.28	4.8	57	1000	89	34
error limits: upper	0.34	NA	64	NA	NA	31
lower	0.20		55			35
300	0.26	4.4	65	1000	91	30
error limits: upper	0.32	NA	68	NA	NA	29
lower	0.20		62			32
250	0.27	5.0	69	1000	92	28
error limits: upper	0.34	NA	72	NA	NA	26
lower	0.10		65			30
200	0.30	4.0	77	1000	94	24
error limits: upper	0.37	NA	80	NA	NA	22
lower	0.15		74			25

The orientational correlation function is assumed to be symmetric about the time origin of the experiment because orientational motion modulates the dynamics of the perturbed free induction decay signal measured at negative time delays, just as it influences the dynamics measured at positive time delays.

Curves corresponding to the best fit from a least-squares fitting procedure employing eq 4 of the parallel and perpendicular polarization traces measured at 300 K are overlaid on the experimental data in Figure 4. The corresponding anisotropy decay obtained from this fitting procedure is overlaid on the anisotropy trace labeled "300 K" in Figure 6. Best fit functions describing with equal fidelity the experimentally measured parallel and perpendicular polarization traces measured at 200, 250, and 350 K (data not shown) are used to obtain the anisotropy decays overlaid on the other anisotropy traces in the Figure 6.

The parameters from the best fit curves for each temperature along with relevant error limits are summarized in Table 2. The error limits were obtained by fixing the parameter in question at a range of values while allowing all other parameters in eq 5 to be optimized such that the sum of the squares of the residuals increased 50% relative to the best fit. We note that the finite vibrational lifetime of the carbonyl stretch mode limits the dynamic range over which we can observe slower orientational motion of the carbonyl group. Consequently, the time constants of the slower orientational components are not accurately determined from the fitting procedure.

Interestingly, the initial anisotropy values obtained from the fitting function are in the range of 0.42−0.44, slightly larger than the value of 0.4 predicted from an initial isotropic distribution of transition dipole moment vectors. The analysis suggests some degree of molecular ordering may exist in the film such that the initial distribution of transition dipole moments interacting with the IR pump pulse is not isotropic. It is also possible that a small nonresonant signal is present in the IR pump−probe signals around the time origin. If this signal were larger with parallel polarizations of the pulses, it could give rise to an artificially high anisotropy measurement, particularly around the time origin.

Figure 7 displays 2D IR spectra of the carbonyl stretch of PCBM measured at 1, 3, and 10 ps following excitation of the 0−1 transition with a narrow-band tunable infrared pump pulse. 2D IR spectra measured at 350 and 200 K are represented. 2D IR spectra were also collected at 250 and 300 K (data not shown). These spectra exhibit the same general features and are of the same data quality as those represented in Figure 7. The two-dimensional spectra contain two frequency axes. The vertical axis, ω_m, results from dispersing the probe beam into a spectrograph. The horizontal axis, ω_p, corresponds to the

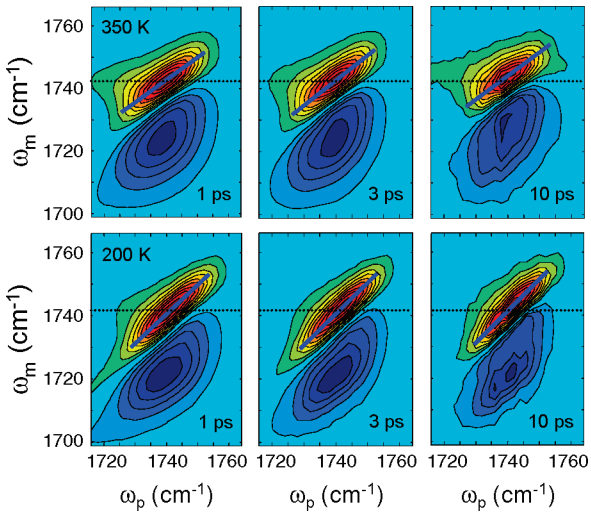

Figure 7. 2D IR spectra measured at 350 and 200 K at time delays of 1, 3, and 10 ps. The center line slopes of the 2D peak shapes appear to be nearly invariant with time within a given temperature. The slight change in peak shape at longer time delays results from excited state population relaxation into the vibrationally hot carbonyl ground state that is centered at higher frequency (see Figure 3B).

frequency of the pump pulse at which a spectrum was recorded with the probe pulse. For all 2D IR spectra collected, a 2 cm^{-1} step between pump frequencies was used. The 2D IR spectra are plotted as change in transmission and are normalized to their maximum positive signal. The contours represent 10% intervals of the maximum positive signal in each spectrum.

Two 2D peak shapes are observed in each spectrum corresponding to the 0−1 and 1−2 transitions of the carbonyl stretch. The 0−1 transitions appear on the diagonals ($\omega_m = \omega_p$) and possess a positive sign because they correspond to the ground state bleach and excited state stimulated emission. Both processes result in increased transmission of the probe. The 1−2 transitions appear shifted off-diagonal along the ω_m axis by the vibrational anharmonicity of 18 cm^{-1} and have a negative sign because they result from the excited state absorption. The anharmonicity observed here is comparable to the value we reported previously.[26] Similar values have been measured for the C═O stretch of methyl acetate in carbon tetrachloride.[30] The 0−1 and 1−2 transitions exhibit different line shapes in the 2D IR spectra because of the anharmonic vibrational potential. Similar behavior has been observed for the amide I band (C═O stretch) of *n*-methylacetamide.[31]

The diagonally elongated shapes of the 0−1 and 1−2 transitions in the $T_w = 1$ ps spectrum indicate that the carbonyl stretch transition is inhomogeneously broadened in the polymer blend. We recently demonstrated that this inhomogeneous broadening results in part from a combination of vibrational solvatochromism and the vibrational Stark effect.[17,18,32] The frequency of the carbonyl group of a PCBM molecule is sensitive to the phase-separated morphology of the polymer blend such that molecules in close contact with conjugated polymers have higher frequency vibrational modes than do molecules in the interiors of PCBM clusters. The variation in environments around PCBM molecules in the polymer blend gives rise to the inhomogeneously broadened vibrational line shapes that appear in Figure 7.

Comparing the 2D IR spectra collected at the same temperature but at different pump−probe time delays, it is apparent that the 2D peak shapes change little on the 10 ps time scale. This observation indicates that C═O oscillators excited by the narrow-band IR pump pulse do not exchange with oscillators having different frequencies, a process known as spectral diffusion.[33,34] Physically, this observation indicates that PCBM molecules in close proximity with CN-MEH-PPV do not exchange with molecules in interior regions of the clusters on the picosecond time scale.[17] It should not be surprising that PCBM molecules do not diffuse on the ultrafast time scale, given that they weigh more than 900 Da and reside in semicrystalline clusters in the polymer blend. Although the 2D vibrational line shapes are essentially time-invariant, the positions of the 0−1 and 1−2 transitions do exhibit a net shift to higher frequency in the 10 ps spectra in comparison to 1 and 3 ps spectra (see the dotted horizontal lines in Figure 7). As we discuss below, this shift arises from formation of the vibrationally hot ground state following excited state relaxation of the carbonyl stretch mode. Finally, the dynamic line widths of the 0−1 and 1−2 transitions of the carbonyl stretch mode (observed as the antidiagonal line widths) do depend on temperature and are larger at 350 K than at 200 K. As we discuss below, this trend correlates with the variation of the wobbling-in-cone angle of the carbonyl groups with temperature. These trends are quantified by detailed analysis procedures that are described below.

Discussion

Linear IR Spectra. The linear IR spectra of the carbonyl group of PCBM displayed in Figure 2 reveal that this vibrational mode is relatively insensitive to temperature. The center frequency shifts 1.5 cm^{-1} to higher values over a factor of 2 change in temperature while the line width changes less than 0.3 cm^{-1}. The relative insensitivity of the carbonyl stretch to temperature contrasts with many vibrational modes examined in other chemical systems.[35−51] For example, the hydroxyl stretch of water and alcohols exhibits marked temperature dependence due to modulation of hydrogen bonding interactions between molecules.[52−54] Similarly, the amide-I vibration of proteins displays significant temperature dependence associated with changes in secondary and tertiary structure.

The sensitivity of these vibrational modes to temperature arises from strong coupling to their environments. Hydrogen bonding interactions between hydroxyl groups of water or alcohols at room temperature give rise to intermolecular interactions with dissociation energies on the order of 20 kJ/mol (0.2 eV).[59−61] The corresponding shallow vibrational potentials give rise to closely spaced vibrational levels of the hydrogen bonding coordinates. As the vibrational occupation of the closely spaced levels vary with temperature, the frequencies of the coupled hydroxyl stretch vibrations change, giving rise to pronounced temperature dependence in the linear IR spectra.

Similarly, the amide I vibration of proteins exhibits significant temperature sensitivity because of their high concentration and strong interactions with the environment.[50,55−58] Amide bonds exist on every protein residue and therefore have high effective concentrations. Their close proximity in conjunction with high intermolecular order present in certain secondary and tertiary structures (α-helices, β-sheets) gives rise to collective vibrations that extend over large regions of proteins.[62] The frequencies of these collective vibrations depend sensitively on protein structure[63,64] through a combination of through-space electrostatic couplings[62,65] and hydrogen bonding interactions.[62,66] Because the structures of proteins are highly temperature-dependent, the vibrational spectra of amide I vibrations display similar sensitivity to temperature.

In contrast to these strongly interacting systems, the carbonyl vibrations in the CN-MEH-PPV:PCBM blend system have comparatively low concentrations and interact weakly with their environment. In particular, the density of pure PCBM is 1.5 g/cm^3, which corresponds to 1.0 molecules/nm^3.[67] The average distance between methyl ester groups of PCBM molecules in PCBM clusters is thus 1 nm, indicating that, on average, the interactions between carbonyl groups are weak. No hydrogen bonding groups are present in the polymer blends, and with the exception of the alkoxy and cyano groups of the polymer, no other polar groups are present. Consequently, the carbonyl groups of PCBM are reasonably well described as dilute, weakly coupled local oscillators such that changes in vibrational occupation of low-frequency modes at various temperatures have limited influence on the vibrational frequencies of the carbonyl groups. The small shift to lower frequency at lower temperature that is observed in Figure 2 is interpreted in terms of enhanced intermolecular order among neighboring carbonyl groups of PCBM molecules. This interpretation is based on the observation of similar shifts to lower frequency with decreased temperature in linear IR spectroscopy studies of the amide I absorption of semicrystalline nylon 11.[68]

The temperature independence of the vibrational line width of the carbonyl group of PCBM suggests that the vibrational dynamics are insensitive to temperature. To investigate this possibility, we examined the temperature dependence of excited state relaxation, orientational diffusion, and spectral diffusion of the carbonyl group of PCBM in the 1:1 polymer blend with CN-MEH-PPV using ultrafast polarization resolved IR pump−probe spectroscopy and two-dimensional IR spectroscopy. In this contribution, we restrict the temperatures over which vibrational dynamics are measured to the 200−350 K range because we wish to compare the results directly to our studies of charge separation in this photovoltaic polymer blend (see ref 14). The following discussion considers the vibrational dynamics in order beginning with excited state relaxation.

Excited State Relaxation Dynamics. In our earlier report on the vibrational dynamics of the carbonyl stretch of PCBM,[26] we interpreted the shift of the frequencies of the 0−1 and 1−2 transitions in the transient vibrational spectra (see Figure 3) in terms of a frequency-dependent vibrational lifetime. Figure 5 displays population relaxation kinetics traces measured at several frequencies around 1740 cm^{-1}. The long time-scale components obtained from the fitting procedure for each wavelength have been subtracted from the kinetics traces to remove the time dependence of this component from the data. The comparison demonstrates that the vibrational dynamics are actually invariant with frequency within experimental precision. The signals follow single-exponential behavior (with a time constant of 1.7 ps) over 2 orders of magnitude decay (more than four time constants). We assign the 1.7 ps component of the population relaxation kinetics to dissipation of vibrational energy out of the carbonyl excited state and into strongly coupled acceptor vibrational modes (see below). Our earlier interpretation of a frequency-dependent lifetime arose from an oversight of the small long-lived decay component in the data.

The spectrum of the long-lived signal subtracted from the kinetics traces displayed in Figure 5 differs slightly in comparison to the spectrum of the initially excited carbonyl stretch mode. The spectrum of the long-lived signal is represented by the 10 ps spectrum in Figure 3B. Because excited state relaxation is essentially complete by 10 ps, we assign the vibrational features in the 10 ps spectrum to a vibrationally hot intermediate state for which the carbonyl stretch mode is in the ground vibrational state. The positive-going feature corresponds to the 0−1 transition of the original ground state that is depleted by excitation of the carbonyl group and subsequent formation of the vibrationally hot intermediate state. We assign the negative going feature to the 0−1 transition of the carbonyl group of the vibrationally hot intermediate state. This feature appears shifted to lower frequency because the carbonyl group is coupled to other vibrational modes that are excited by dissipation of vibrational energy out of the carbonyl stretch. Destructive interference between the 0−1 transition of the vibrationally hot intermediate state and the 0−1 transition of the original ground state causes the positive-going signal in the 10 ps spectrum to appear shifted to higher frequency. Finally, the vibrationally hot intermediate state decays to the thermalized ground state on the >10 ps time scale.

The semilogarithmic plot of the population relaxation kinetics traces of the carbonyl stretch of PCBM in Figure 5 emphasizes the biphasic nature of the vibrational relaxation dynamics. About 40% of the excited state population decays on the 300 fs time scale, and the remainder of the population relaxation occurs on the 1.7 ps time scale (see Table 1, 300 K). Similar biphasic excited state relaxation dynamics were reported by Tokmakoff and co-workers in the amide I vibration of *n*-methylacetamide.[31] The biphasic behavior was rationalized in terms of rapid exchange of vibrational energy between the strongly coupled amide I and amide II vibrations of the amide functional group on the subpicosecond time scale followed by dissipation of the vibrational energy into the vibrational modes of the bath on the picosecond time scale. The carbonyl stretch of the amide and ester functional groups probably share similar intramolecular coupling to their respective low frequency vibrational modes. Consequently, it is likely that the carbonyl stretch of PCBM undergoes biphasic excited state relaxation due to similar intramolecular vibrational energy redistribution. It is the dissipation of the vibrational energy on the picosecond time scale into the acceptor modes that gives rise to the formation of the vibrationally hot intermediate state whose vibrational features are observed in the 10 ps transient spectrum in Figure 3B.

The best fit parameters of the population relaxation kinetics traces represented in Table 1 reveal that the excited state relaxation dynamics are weakly temperature-dependent. The most pronounced temperature dependence appears in the picosecond decay assigned to the dissipation of vibrational energy into the strongly coupled acceptor modes. Apparently, the vibrational occupation and coupling of the low frequency modes are slightly sensitive to the thermal energy available from the ambient surroundings.

Orientational Relaxation Dynamics. We previously reported wobbling-in-cone orientational motion of the carbonyl stretch vibration of the methyl ester group of PCBM on the few hundred femtosecond time scale at room temperature.[26] Orientational motion of molecular vibrational modes often gives rise to spectral diffusion in liquids because the frequencies of vibrational modes are sensitive to their local solvent environments.[69−71] As the transition dipole moments reorient, they sample different regions of the local environment with associated changes of vibrational frequencies. We anticipate similar behavior in solids such as the CN-MEH-PPV:PCBM blend under consideration in this work. Because the wobbling-in-cone orientational motion is complete on the subpicosecond time scale, this motion does not give rise to spectral diffusion of the carbonyl stretch mode on the picosecond and longer time scale at room temperature.[26] However, if this motion occurs diffusively, then its time scale may be temperature-dependent. We considered the possibility

that this motion may slow sufficiently to cause spectral diffusion on the picosecond time scale, particularly at low temperature. Below, we examine this issue and show that the time scale of orientational motion is, indeed, independent of temperature.

Comparison of the orientational relaxation dynamics measured at different temperatures in Figure 6 (with best fit parameters summarized in Table 2) reveals that the time scale for wobbling-in-cone orientational motion of the carbonyl groups of PCBM, τ_w, does not vary with temperature within experimental precision. This observation indicates that reorientation of the carbonyl group on the subpicosecond time scale occurs through inertial motion with a negligible activation barrier in comparison to the available thermal energy. The procedure to fit the anisotropy data using eqs 4 and 5 characterizes the fast wobbling-in-cone orientational motion with an exponential component of relative amplitude, $1 - Q^2$. In eq 5, Q^2 is a generalized order parameter that characterizes the half angle of the cone, θ, in which the carbonyl bonds undergo ultrafast reorientation. The cone half angle is related to Q^2 according to[24]

$$Q^2 = \left[\frac{1}{2}(\cos\theta)(1 + \cos\theta)\right]^2 \quad (6)$$

Interestingly, the cone half angle is temperature-dependent, varying from 24° at 200 K to 34° at 350 K (see Table 2). The larger half angle indicates an increase in free volume surrounding the PCBM molecules associated with a decrease in the density of the material at higher temperature.[27]

Spectral Diffusion Dynamics. Inspection of the 2D IR spectra displayed in Figure 7 demonstrates qualitatively that little or no spectral diffusion occurs in the carbonyl stretch mode of PCBM on the 10 ps time scale at either 350 or 200 K. To quantify the spectral diffusion dynamics, we adopted two analysis procedures: the first developed by Fayer and co-workers is known as the center line slope method,[72] and the second examines the variation of the dynamic line widths of the 0−1 transitions of the carbonyl stretch.

The idea underpinning the center line slope method is that when the dynamic line width of a particular subensemble of an inhomogeneous distribution of oscillators is much smaller than the inhomogeneous line width, then the peak shapes in the 2D spectra appear elongated along the diagonal with a slope that is near unity. As the subensembles interconvert, giving rise to spectral diffusion, their dynamic line widths increase relative to the inhomogeneous width such that the peaks evolve toward shapes that are symmetric with respect to reflection along the ω_p frequency axis. These changes can be conveniently quantified by the variation of the center line slopes of 2D peak shapes. The center line slopes of the 0−1 transitions of the carbonyl stretch are represented as the solid diagonal lines in Figure 7. The inverse of the center line slope (called the CLS) initially has a value near unity before spectral diffusion occurs. For systems that undergo spectral diffusion, the CLS decays to zero with increased time delay.[72,73]

It was recently shown that the CLS of 2D peak shapes in 2D IR spectra correlate closely with the frequency−frequency correlation functions (FFCF) of the corresponding vibrational transitions.[72]

$$C(t) = \langle \delta\omega(t)\, \delta\omega(0) \rangle \quad (7)$$

The time variance of $C(t)$ describes the joint probability distribution that an oscillator has a particular frequency at time, $t = 0$, and a different frequency at a later time, $t = t'$. The FFCF of the carbonyl stretch determines the time scale for spectral diffusion that is observed in ultrafast vibrational spectroscopy experiments. As such, we are interested in evaluating the time variance of the CLS of the 0−1 transition of the carbonyl stretch of PCBM to determine whether spectral diffusion due to equilibrium fluctuations might give rise to spectral evolution of the carbonyl bleach peak on the picosecond time scale in ultrafast visible pump-IR probe experiments.[14−16]

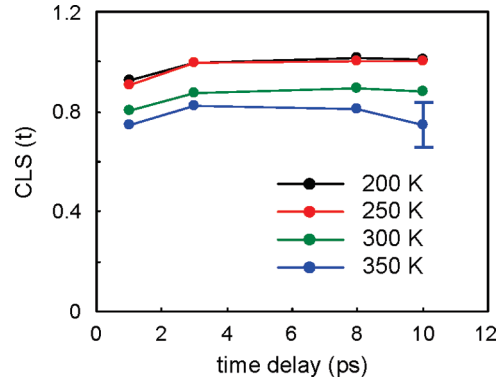

Figure 8. Center line slopes (CLS) obtained from fitting the 2D IR spectra of the carbonyl stretch of PCBM with 2D Gaussian peak shapes. Spectral diffusion of the carbonyl oscillators would cause the value of the CLS to approach zero with increasing time delay. The data indicate negligible spectral diffusion on the 10 ps time scale.

To obtain the time dependence CLS, the 0−1 and 1−2 transitions in the 2D IR spectra were fit with 2D Gaussian peak shapes using a least-squares fitting procedure. The angles at which the Gaussian line shapes are elongated to best describe the peak shapes provide convenient measures of the CLS. Figure 8 depicts the variation of the CLS of the carbonyl stretch 0−1 transition versus the corresponding pump−probe time delay for temperatures of 350, 300, 250, and 200 K. The 2D IR spectra that were fit to obtain the center line slopes at 350 and 200 K are displayed in Figure 7. The spectra from which the center line slopes at 300 and 250 K were measured (data not shown) are of equal quality and have similar vibrational features as the data that are shown in Figure 7. The data reveal that the CLS of the carbonyl stretch of PCBM is essentially time invariant between 1 and 10 ps at all temperatures examined. The small variations in the value of the CLS at different time delays are not significant within the experiment precision indicated by the error bar in Figure 8. The error bar was determined by fixing the angle of the 2D Gaussian peak shape describing the 0−1 transition in a particular 2D IR spectrum and varying all other parameters such that the sum of the squares of the residuals increased 50% relative to the best fit. The error bar is representative of the error bars from all 2D IR spectra.

Taking the time dependence of the CLS in Figure 8 to reflect the time dependence of the FFCF of the carbonyl stretch of PCBM,[72] we find that the FFCF decays little between 1 and 10 ps. This result indicates that thermal fluctuations at the temperatures examined do not give rise to significant frequency fluctuations of the carbonyl stretch of PCBM. To look further for potential evidence of spectral diffusion, dynamic line widths of the 0−1 transition were examined in transient spectra following excitation with the narrow-band IR pump pulse. Figure 9A represents transient vibrational spectra measured at 350 K with the 8 cm^{-1} fwhm IR pump pulse centered at 1740 cm^{-1}. Spectra with pump−probe delays of 1, 3, 8, and 10 ps are represented. The transient spectra at 1 and 3 ps are indistinguishable, indicating that the dynamic line width does

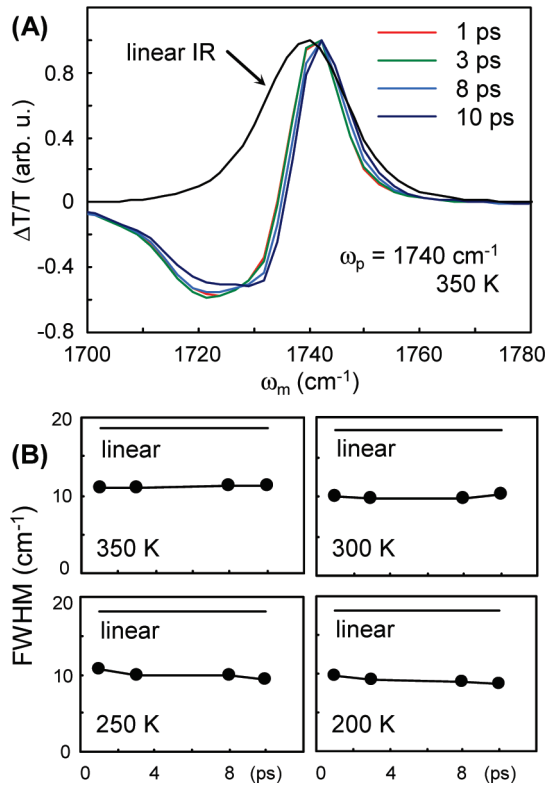

Figure 9. (A) Comparison of transient absorption spectra measured along the ω_m frequency axis at 350 K with a narrow-band IR pump pulse at $\omega_p = 1740$ cm^{-1} at various time delays. (B) Plot of the full width at half-maximum (fwhm) of the dynamic line width of the 0−1 transition (circles) versus the time delay for several temperatures. The line labeled "linear" represents the fwhm of the linear IR absorption spectrum at each temperature. The dynamic line width of the 0−1 transition shows negligible change with increasing time delay, indicating that spectral diffusion is not significant in this system on the 10 ps time scale.

not increase on this time scale. The transient spectra at 8 and 10 ps exhibit a shift to higher frequency resulting from excited state relaxation to the vibrationally hot carbonyl stretch ground state (see Figure 3B). Transient vibrational spectra measured at 300, 250, and 200 K (data not shown) have an appearance essentially identical to those measured at 350 K.

To quantify changes in the dynamic line width at various pump−probe delays, we fit the transient spectra measured with $\omega_p = 1740$ cm^{-1} at all time delays and temperatures with Gaussian line shapes for the 0−1 and 1−2 transitions. The time and temperature dependence of the fwhm of the best fit Gaussian line shapes for the 0−1 transition are represented in Figure 9B. For comparison, the fwhm of the linear IR absorption spectrum of the carbonyl stretch of PCBM in the polymer blend at the indicated temperature is represented in each panel (horizontal lines labeled 'linear'). If spectral diffusion occurred on the 10 ps time scale, the fwhm of the dynamic line width would *increase* toward the value of the linear IR absorption spectrum. The data confirm the conclusion from the CLS analysis that spectral diffusion is not significant on the 10 ps time scale in this polymer blend at all temperatures examined.

It is interesting to note that although the shapes of the 0−1 and 1−2 transitions in Figure 7 undergo negligible changes due to spectral diffusion, their center frequencies do change with time. Close inspection of the centers of the 0−1 transitions in the 2D IR spectra recorded at 10 ps time delay reveals that the center frequencies of these peaks shift to higher values by about 2 cm^{-1}, the same magnitude of frequency shift that is observed in the transient vibrational spectra displayed in Figure 3B. The frequency shifts have the same origin: formation of the vibrationally hot intermediate state following excited state relaxation of the carbonyl stretch mode. The fact that the precise frequency of a carbonyl stretch mode initially excited by the IR pump pulse is preserved through the vibrational relaxation and dissipation processes is fascinating and is a manifestation of the inhomogeneous broadening mechanism in this system.

We recently demonstrated that the frequencies of carbonyl groups of PCBM molecules in close contact with conjugated polymers have higher-frequency vibrational modes than do molecules in the interiors of PCBM clusters (see Figure 1C).[17,18,32] The variation in vibrational frequency results from a combination of vibrational solvatochromism[19] and the vibrational Stark effect.[20,21] This inhomogeneous broadening mechanism indicates that for PCBM molecules to sample frequencies outside of their dynamic line widths (and thus undergo spectral diffusion), they must diffuse toward or away from PCBM/CN-MEH-PPV interfaces. Center of mass motion of PCBM molecules is expected to be extremely slow because of their large molar mass and their tendency to form semicrystalline clusters in the polymer blend. This motion is not expected to be influenced by the formation of vibrationally hot intermediate states as a result of vibrational relaxation of the initially excited carbonyl stretch mode. Thus, it is reasonable to expect that spectral diffusion in the carbonyl stretch would not occur even after vibrational relaxation in this chemical system. In total, these observations support our earlier interpretation of the frequency shift dynamics of the carbonyl stretch mode of PCBM following ultrafast visible excitation exclusively in terms of charge separation.[14−18]

Finally, we note that the variation of the CLS versus temperature in Figure 8 corresponds closely to the temperature dependence of the cone half angle of the wobbling-in-cone orientational motion calculated from the anisotropy data depicted in Figure 6. An increase in the cone half angle from 24° to 34° corresponds to a decrease of the CLS from near unity to ~0.8. The dynamic line width increases from about 9 cm^{-1} to about 11 cm^{-1} during the same temperature change. This observation indicates that the dynamic line width of the carbonyl stretch of PCBM is strongly influenced by orientational motion of the methyl ester group. Furthermore, we predict that spectral diffusion would be observed in the carbonyl stretch of PCBM if the sample were cooled sufficiently to slow the wobbling-in-cone orientational motion into the picosecond time scale or if 2D IR spectra were collected with the 3-pulse photon echo technique having sub-100 fs time resolution.

Conclusion

Temperature-dependent measurements using ultrafast vibrational spectroscopy to study the carbonyl stretch of the functionalized fullerene, PCBM, in a blend with the conjugated polymer, CN-MEH-PPV, reveal that the vibrational dynamics are nearly invariant with temperature. The time scales of vibrational excited state relaxation and wobbling-in-cone orientational motion do not change between 200 and 350 K. Spectral diffusion is not observed on the 1−10 ps time scale at all temperatures examined. However, the half angle of wobbling-in-cone orientational motion and the dynamic line width of the carbonyl stretch do depend on temperature. This dependence arises from changes in the density of the polymer blend due to thermal expansion at elevated temperatures.

The observations reported here indicate that the carbonyl stretch of the methyl ester groups of PCBM are well described

as dilute weakly coupled local modes that experience essentially static solvent environments. The corresponding static inhomogeneity of the distribution of carbonyl stretch frequencies makes the carbonyl group an ideal vibrational probe of charge carrier dynamics in the polymer blend. In total, the observations reported here substantiate our earlier report of activationless charge separation in this polymer blend on the basis of a temperature-dependent study of the photoinduced time evolution of the vibrational spectra of the carbonyl stretch of PCBM.[14−16]

Acknowledgment. This material is based upon work supported by the National Science Foundation under Grant No. 0846241, the Henry Dreyfus New Faculty Awards Program, and the 3M Corporation Non-Tenured Faculty Award Program.

References and Notes

(1) Thompson, B. C.; Frechet, J. M. J. *Angew. Chem., Int. Ed.* **2008**, *47*, 58.
(2) Gunes, S.; Neugebauer, H.; Sariciftci, N. S. *Chem. Rev.* **2007**, *107*, 1324.
(3) Gregg, B. A. *Mat. Res. Soc. Bull.* **2005**, *30*, 20.
(4) Clarke T. M.; Durrant J. R. *Chem. Rev.* **2010**, *110*, DOI: 10.1021/CR900271S.
(5) Bredas, J.-L.; Norton, J. E.; Cornil, J.; Coropceanu, V. *Acc. Chem. Res.* **2009**, *42*, 1691.
(6) Ohkita, H.; Cook, S.; Astuti, Y.; Duffy, W.; Tierney, S.; Zhang, W.; Heeney, M.; McCulloch, I.; Nelson, J.; Bradley, D. D. C.; Durrant, J. R. *J. Am. Chem. Soc.* **2008**, *130*, 3030.
(7) Clarke, T.; Ballantyne, A.; Jamieson, F.; Brabec, C.; Nelson, J.; Durrant, J. *Chem. Commun.* **2009**, 89.
(8) Veldman, D.; Ipek, O.; Meskers, S. C. J.; Sweelssen, J.; Koetse, M. M.; Veenstra, S. C.; Kroon, J. M.; van Bavel, S. S.; Loos, J.; Janssen, R. A. J. *J. Am. Chem. Soc.* **2008**, *130*, 7721.
(9) Mandoc, M. M.; Veurman, W.; Sweelssen, J.; Koetse, M. M.; Blom, P. M. W. *Appl. Phys. Lett.* **2007**, *91* (3), 073518.
(10) Veldman, D.; Meskers, S. C. J.; Janssen, R. A. J. *Adv. Funct. Mater.* **2009**, *19*, 1939.
(11) Muntwiler, M.; Yang, Q.; Tisdale, W. A.; Zhu, X.-Y. *Phys. Rev. Lett.* **2008**, *101* (4), 196403.
(12) Gregg, B. A.; Chen, S.-G.; Cormier, R. A. *Chem. Mater.* **2004**, *16*, 4586.
(13) Peumans, P.; Forrest, S. R. *Chem. Phys. Lett.* **2004**, *398*, 27.
(14) Pensack, R. D.; Asbury, J. B. *J. Am. Chem. Soc.* **2009**, *131*, 15986.
(15) Pensack R. D.; Banyas K. M.; Asbury J. B. *IEEE J. Select. Topics Quan. Elec.* **2010**, DOI: 10.1109/JSTQE.2010.2041751.
(16) Pensack, R. D.; Asbury, J. B. *J. Phys. Chem. Lett.* **2010**, *1*, 2255.
(17) Barbour, L. W.; Hegadorn, M.; Asbury, J. B. *J. Am. Chem. Soc.* **2007**, *129*, 15884.
(18) Pensack, R. D.; Banyas, K. M.; Barbour, L. W.; Hegadorn, M.; Asbury, J. B. *Phys. Chem. Chem. Phys.* **2009**, *11*, 2575.
(19) Cho, M. *J. Chem. Phys.* **2009**, *130* (15), 094505.
(20) Park, E. S.; Boxer, S. G. *J. Phys. Chem. B* **2002**, *106*, 5800.
(21) Boxer, S. G. *J. Phys. Chem. B* **2009**, *113*, 2972.
(22) Barbour, L. W.; Pensack, R. D.; Hegadorn, M.; Arzhantsev, S.; Asbury, J. B. *J. Phys. Chem. C* **2008**, *112*, 3926.
(23) Pensack, R. D.; Banyas, K. M.; Asbury, J. B. *J. Phys. Chem. C* **2010**, *114*, 5344.
(24) Lipari, G.; Szabo, A. *Biophys. J.* **1980**, *30*, 489.
(25) Wang, C. C.; Pecora, R. *J. Chem. Phys.* **1980**, *72*, 5333.
(26) Barbour, L. W.; Hegadorn, M.; Asbury, J. B. *J. Phys. Chem. B* **2006**, *110*, 24281.
(27) *Polymer Handbook*; 4th ed.; Brandrup, J., Immergut, E. H., Grulke, E. A., Eds.; John Wiley & Sons: New York, 1999.
(28) Tan, H.-S.; Piletic, I. R.; Fayer, M. D. *J. Opt. Soc. Am. B* **2005**, *22*, 2009.
(29) Hamm, P.; Lim, M.; DeGrado, W. F.; Hochstrasser, R. M. *J. Chem. Phys.* **2000**, *112*, 1907.
(30) Lim, M.; Hochstrasser, R. M. *J. Chem. Phys.* **2001**, *115*, 7629.
(31) DeFlores, L. P.; Ganim, Z.; Ackley, S. F.; Chung, H. S.; Tokmakoff, A. *J. Phys. Chem. B* **2006**, *110*, 18973.
(32) Pensack, R. D.; Banyas, K. M.; Hegadorn, M.; Asbury, J. B. *Phys. Chem. Chem. Phys.* **2010**, DOI: 10.1039/C0CP00971G.
(33) Asbury, J. B.; Steinel, T.; Stromberg, C.; Corcelli, S. A.; Lawrence, C. P.; Skinner, J. L.; Fayer, M. D. *J. Phys. Chem. A* **2004**, *108*, 1107.
(34) Tokmakoff, A.; Urdahl, R. S.; Zimdars, D.; Francis, R. S.; Kwok, A. S.; Fayer, M. D. *J. Chem. Phys.* **1995**, *102*, 3919.
(35) Bakker, H. J.; Skinner, J. L. *Chem. Rev.* **2010**, *110*, 1498.
(36) Smits, M.; Ghosh, A.; Sterrer, M.; Muller, M.; Bonn, M. *Phys. Rev. Lett.* **2007**, *98* (4), 098302.
(37) Deak, J. C.; Pang, Y.; Sechler, T. D.; Wang, Z.; Dlott, D. D. *Science* **2004**, *306*, 473.
(38) Szyc, L.; Yang, M.; Nibbering, E. T. J.; Elsaesser, T. *Angew. Chem., Int. Ed.* **2010**, *49*, 3598.
(39) Moilanen, D. E.; Wong, D.; Rosenfeld, D. E.; Fenn, E. E.; Fayer, M. D. *Proc. Natl. Acad. Sci. U.S.A.* **2009**, *106*, 375.
(40) Eaves, J. D.; Loparo, J. J.; Fecko, C. J.; Roberts, S. T.; Tokmakoff, A.; Geissler, P. L. *Proc. Nat. Acad. Sci.* **2005**, *102*, 13019.
(41) Moore, F. G.; Richmond, G. L. *Acc. Chem. Res.* **2008**, *41*, 739.
(42) Suydam, I. T.; Snow, C. D.; Pande, V. S.; Boxer, S. G. *Science* **2006**, *313*, 200.
(43) Fayer, M. D. *Annu. Rev. Phys. Chem.* **2009**, *60*, 21.
(44) Du, D.; Bunagan, M. R.; Gai, F. *Biophys. J.* **2007**, *93*, 4076.
(45) Maekawa, H.; De Poli, M.; Toniolo, C.; Ge, N.-H. *J. Am. Chem. Soc.* **2009**, *131*, 2042.
(46) Bredenbeck, J.; Helbing, J.; Nienhaus, K.; Nienhaus, G. U.; Hamm, P. *Proc. Natl. Acad. Sci. U.S.A.* **2007**, *104*, 14243.
(47) Rubstov, I. V.; Wang, J.; Hochstrasser, R. M. *Proc. Natl. Acad. Sci. U.S.A.* **2003**, *100*, 5601.
(48) Keiderling, T. A. *Curr. Opin. Chem. Biol.* **2002**, *6*, 682.
(49) Rubtsov, I. V. *Acc. Chem. Res.* **2009**, *42*, 1385.
(50) Ganim, Z.; Chung, H. S.; Smith, A. W.; Deflores, L. P.; Jones, K. C.; Tokmakoff, A. *Acc. Chem. Res.* **2008**, *41*, 432.
(51) Shim, S.-H.; Strasfeld, D. B.; Ling, Y. L.; Zanni, M. T. *Proc. Natl. Acad. Sci. U.S.A.* **2007**, *104*, 14197.
(52) Fishman, E.; Saumagne, P. *J. Phys. Chem.* **1965**, *69*, 3671.
(53) Falk, M.; Ford, T. A. *Can. J. Chem.* **1966**, *44*, 1699.
(54) Libnau, F. O.; Toft, J.; Christy, A. A.; Kvalheim, O. M. *J. Am. Chem. Soc.* **1994**, *116*, 8311.
(55) Wang, J.; El-Sayed, M. A. *Biophys. J.* **1999**, *76*, 2777.
(56) Fabian, H.; Schultz, C.; Naimann, D.; Landt, O.; Hahn, U.; Saenger, W. *J. Mol. Biol.* **1993**, *232*, 967.
(57) Reinstadler, D.; Fabian, H.; Backmann, J.; Naumann, D. *Biochemistry* **1996**, *35*, 15822.
(58) Chung, H. S.; Khalil, M.; Smith, A. W.; Ganim, Z.; Tokmakoff, A. *Proc. Nat. Acad. Sciences USA* **2005**, *102*, 612.
(59) Solomonov, B. N.; Novikov, V. B.; Varfolomeev, M. A.; Klimovitskii, A. E. *J. Phys. Org. Chem.* **2005**, *18*, 1132.
(60) Khan, A. *J. Phys. Chem. B* **2000**, *104*, 11268.
(61) Suresh, S. J.; Naik, V. M. *J. Chem. Phys.* **2000**, *113*, 9727.
(62) Krimm, S.; Bandekar, J. *Adv. Protein Chem.* **1986**, *38*, 181.
(63) Gilmanshin, R.; Williams, S.; Callender, R. H.; Woodruff, W. H.; Dyer, R. B. *Proc. Natl. Acad. Sci. U.S.A.* **1997**, *94*, 3709.
(64) Dyer, R. B.; Gai, F.; Woodruff, W. H.; Gilmanshin, R.; Callender, R. H. *Acc. Chem. Res.* **1998**, *31*, 709.
(65) Hamm, P.; Lim, M.; Hochstrasser, R. M. *J. Phys. Chem. B* **1998**, *102*, 6123.
(66) McDowell, L. M.; Kirmaier, C.; Holten, D. *J. Phys. Chem.* **1991**, *95*, 3379.
(67) Bulle-Lieuwma, C. W. T.; van Gennip, W. J. H.; van Duren, J. K. J.; Jonkheijm, P.; Jannsen, R. A. J.; Niemantsverdriet, J. W. *Appl. Surf. Sci.* **2003**, *203*, 547.
(68) Skrovanek, D. J.; Painter, P. C.; Coleman, M. M. *Macromolecules* **1986**, *19*, 699.
(69) Park, S.; Fayer, M. D. *Proc. Natl. Acad. Sci. U.S.A.* **2007**, *104*, 16731.
(70) Lawrence, C. P.; Skinner, J. L. *J. Chem. Phys.* **2003**, *118*, 264.
(71) Fecko, C. J.; Loparo, J. J.; Roberts, S. T.; Tokmakoff, A. *J. Chem. Phys.* **2005**, *122* (18), 054506.
(72) Kwak, K.; Park, S.; Finkelstein, I. J.; Fayer, M. D. *J. Chem. Phys.* **2007**, *127* (17), 124503.
(73) Park, S.; Moilanen, D. E.; Fayer, M. D. *J. Phys. Chem. B* **2008**, *112*, 5279.

JP105772Y